

Channel state information estimation for 5G wireless communication systems: Recurrent neural networks approach

Mohamed Hassan Ali ^{Corresp., 1}, Ibrahim B. M. Taha ²

¹ Department of Electrical Engineering, Faculty of Engineering, Al-Azhar University,, 1Department of Electrical Engineering, Faculty of Engineering, Al-Azhar University, Qena 83513, Egypt, Qena, Qena, Egypt

² Department of Electrical Engineering, College of Engineering,, Taif University, Taif 21944,, Saudi Arabia, Taif, Taif

Corresponding Author: Mohamed Hassan Ali
Email address: mhessai@azhar.edu.eg

In this study, a deep learning bidirectional long short-term memory (BiLSTM) recurrent neural network-based channel state information estimator is proposed for 5G orthogonal frequency-division multiplexing systems. The proposed estimator is a pilot-dependent estimator and follows the online learning approach in the training phase and the offline approach in the practical implementation phase. The estimator does not deal with complete a priori certainty for channels' statistics and attains superior performance in the presence of a limited number of pilots. A comparative study is conducted using three loss functions, namely, mean absolute error, cross entropy function for k th mutually exclusive classes and sum of squared of the errors. The Adam optimisation algorithm is used to evaluate the performance of the proposed estimator under each loss function. In terms of symbol error rate and accuracy metrics, the proposed estimator outperforms long short-term memory (LSTM) neural network-based channel state information, least squares and minimum mean square error estimators under different simulation conditions. The computational and training time complexities for deep learning BiLSTM- and LSTM-based estimators are provided. Given that the proposed estimator relies on the deep learning neural network approach, where it can analyse massive data, recognise statistical dependencies and characteristics, develop relationships between features and generalise the accrued knowledge for new datasets that it has not seen before, the approach is promising for any 5G and beyond communication system.

1 Channel State Information Estimation for 5G Wireless 2 Communication Systems: Recurrent Neural Networks 3 Approach

4
5

6 Mohamed Hassan Essai Ali¹ and Ibrahim B. M. Taha²

7
8

9 ¹Department of Electrical Engineering, Faculty of Engineering, Al-Azhar University, Qena
10 83513, Egypt

11 ²Department of Electrical Engineering, College of Engineering, Taif University, Taif 21944,
12 Saudi Arabia

13
14

15 Corresponding Author:

16 Mohamed Hassan Essai Ali ¹

17 Masaken Osman, Qena, Qena, 83513, Egypt

18 Email address: mhessai@azhar.edu.eg

19
20

20 Abstract

21 In this study, a deep learning bidirectional long short-term memory (BiLSTM) recurrent neural
22 network-based channel state information estimator is proposed for 5G orthogonal frequency-
23 division multiplexing systems. The proposed estimator is a pilot-dependent estimator and follows
24 the online learning approach in the training phase and the offline approach in the practical
25 implementation phase. The estimator does not deal with complete a priori certainty for channels'
26 statistics and attains superior performance in the presence of a limited number of pilots. A
27 comparative study is conducted using three classification layers that use loss functions: mean
28 absolute error, cross entropy function for kth mutually exclusive classes and sum of squared of the
29 errors. The Adam, RMSProp, SGdm, and Adadelat optimisation algorithms are used to evaluate
30 the performance of the proposed estimator using each classification layer. In terms of symbol error
31 rate and accuracy metrics, the proposed estimator outperforms long short-term memory (LSTM)
32 neural network-based channel state information, least squares and minimum mean square error
33 estimators under different simulation conditions. The computational and training time
34 complexities for deep learning BiLSTM- and LSTM-based estimators are provided. Given that the
35 proposed estimator relies on the deep learning neural network approach, where it can analyse
36 massive data, recognise statistical dependencies and characteristics, develop relationships between
37 features and generalise the accrued knowledge for new datasets that it has not seen before, the
38 approach is promising for any 5G and beyond communication system.

39

40 Introduction

41 5G wireless communication is the most active area of technology development and a rapidly
42 growing branch of the wider field of communication systems. Wireless communication has made
43 various possible services ranging from voice to multimedia.

44 The physical characteristics of the wireless communication channel and many unknown
45 surrounding effects result in imperfections in the transmitted signals. For example, the transmitted
46 signals experience reflections, diffractions, and scattering, which produce multipath signals with
47 different delays, phase shift, attenuation, and distortion arriving at the receiving end; hence, they
48 adversely affect the recovered signals (Oyerinde & Mneney 2012b).

49 A priori information on the physical characteristics of the channel provided by pilots is one of
50 the significant factors that determine the efficiency of channel state information estimators
51 (CSIEs). For instance, if not a priori information is available (no or insufficient pilots), channel
52 estimation is useless; finding what you do not know is impossible. When complete information on
53 the transmission channel is available, CSIEs are no longer needed. Thus, a priori uncertainty exists
54 for communication channel statistics. However, the classical theory of detection, recognition, and
55 estimation of signals deals with complete priory certainty for channel statistics, and it is an
56 unreliable and unpractical assumption (Bogdanovich et al. 2009).

57 In the classic case, uncertainty is related to useful signals. In detection problems, the unknown
58 is the fact of a signal existence. In recognition problems, the unknown is the type of signal being
59 received at the current moment. In estimation problems, the unknown is the amplitude of the
60 measured signal or one of its parameters. The rest of the components of the signal-noise
61 environment in classical theory are regarded as a priori certain (known) as follows: the known is
62 the statistical description of the noise, the known is the values of the unmeasured parameters of
63 the signal and the known is the physical characteristics of the wireless communication channel. In
64 such conditions, the classical theory allows the synthesis of optimal estimation algorithms, but the
65 structure and quality coefficients of the algorithms depend on the values of the parameters of the
66 signal-noise environment. If the values of the parameters describing the signal-noise environment
67 are slightly different from the parameters for which the optimal algorithm is built, then the quality
68 coefficients will become substantially poor, making the algorithm useless in several cases
69 (Bogdanovich et al. 2009), (O'Shea et al. 2017). The most frequently used CSIEs are derived from
70 signal and channel statistical models by employing techniques, such as maximum likelihood (ML),
71 least squares (LS), and minimum mean squared error (MMSE) optimisation metrics (Kim 2015).

72 One of the major concerns in the optimum performance of wireless communication systems is
73 providing accurate channel state information (CSI) at the receiver end of the systems to detect the
74 transmitted signal coherently. If CSI is unavailable at the receiver end, then the transmitted signal
75 can only be demodulated and detected by a noncoherent technique, such as differential
76 demodulation. However, using a noncoherent detection method occurs at the expense of a loss of
77 signal-to-noise ratio of about 3–4 dB compared with using a coherent detection technique. To
78 eliminate such losses, researchers have focused on the development of channel estimation
79 techniques to provide perfect detection of transmitted information in wireless communication
80 systems using the Orthogonal Frequency-Division Multiplexing (OFDM) modulation scheme
81 (Oyerinde & Mneney 2012a).

82 The use of deep learning neural networks (DLNNs) is the state-of-the-art approach in the field
83 of wireless communication. The amazing learning capabilities of DLNNs from training data sets
84 and the tremendous progress of graphical processing units (GPUs), which are considered the most
85 powerful tools for training DLNNs, have motivated its usage for different wireless communication
86 issues, such as modulation recognition (Zhou et al. 2020), (Karra et al. 2017) and channel state
87 estimation and detection (Essai Ali ; Joo et al. 2019; Kang et al. 2020; Ma et al. 2018; Ponnaluru
88 & Penke 2020; Yang et al. 2019a; Ye et al. 2018). According to (Karra et al. 2017; Kim 2015;
89 Oyerinde & Mneney 2012a; Zhou et al. 2020) and (Ma et al. 2018), all proposed deep learning-
90 based CSIEs have better performance compared with the examined traditional channel ones, such
91 as LS and MMSE estimators.

92 Recently, numerous long short-term memory (LSTM)- and BiLSTM-based applications have
93 been introduced for prognostic and health management (Zhao et al. 2020), artificial intelligence-
94 based translation systems (Wu et al. 2016), (Ong 2017) and other areas. For channel state
95 information estimation in 5G-OFDM wireless communication systems, many deep learning
96 approaches, such as convolutional neural network (CNN), recurrent neural network (RNN) (e.g.
97 LSTM and BiLSTM NNs) and hybrid (CNN and RNN) neural networks have been used (Essai Ali
98 ; Liao et al. 2019; Luo et al. 2018b; Ponnaluru & Penke 2020; Yang et al. 2019a; Yang et al. 2019b;
99 Ye et al. 2018).

100 In (Liao et al. 2019), a deep learning-based CSIE was proposed by using CNN and BiLSTM-
101 NN for the extraction of the feature vectors of the channel response and channel estimation,
102 respectively. The aim was to improve the channel state information estimation performance at the
103 downlink, which is caused by the fast time-varying and varying channel statistical characteristics
104 in high-speed mobility scenarios. In (Luo et al. 2018a), an online-trained CSIE that is an integration
105 of CNN and LSTM-NN was proposed. The authors also developed an offline–online training
106 technique that applies to 5G wireless communication systems. In (Ye et al. 2018), a joint channel
107 estimator and detector that is based on feedforward DLNNs for frequency selective channel
108 (OFDM) systems was introduced. The proposed algorithm was found to be superior to the
109 traditional MMSE estimation method when unknown surrounding effects of communication
110 systems are considered. In (Yang et al. 2019a), an online estimator was developed by adopting
111 feedforward DLNNs for doubly selective channels. The proposed estimator was considered
112 superior to the traditional LMMSE estimator in all investigated scenarios. In (Ponnaluru & Penke
113 2020), a one-dimensional CNN (1D-CNN) deep learning estimator was proposed. Under various
114 modulation scenarios and in terms of MSE and BER metrics, the authors compared the
115 performance of the proposed estimator with that of feedforward neural networks (FFNN), MMSE
116 and LS estimators. 1D-CNN outperformed LS, MMSE and FFNN estimators. In (Essai Ali), an
117 online pilot-assisted estimator model for OFDM wireless communication systems was developed
118 by using LSTM NN. The conducted comparative study showed the superior performance of the
119 proposed estimator in comparison with LS and MMSE estimators under limited pilots and a prior
120 uncertainty of channel statistics. The authors in (Sarwar et al. 2020) used the genetic algorithm-
121 optimised artificial neural network to build a CSIE. The proposed estimator was dedicated for
122 space–time block-coding MIMO-OFDM communication systems. The proposed estimator
123 outperformed LS and MMSE estimators in terms of BER at high SNRs, but it achieved
124 approximately the same performance as LS and MMSE estimators at low SNRs. The authors in
125 (Senol et al. 2021) proposed a CSIE for OFDM systems by using ANN under the condition of
126 sparse multipath channels. The proposed estimator achieved a comparable SER performance as
127 matching pursuit- and orthogonal matching pursuit-based estimators at a lower computational
128 complexity than that of the examined estimators. The authors in (Le Ha et al. 2021) proposed a
129 CSIE that uses deep learning and LS estimator and utilizes the multiple-input multiple-output
130 system for 5G-OFDM. The proposed estimator minimizes the MSE loss function between the LS-
131 based channel estimation and the actual channel. The proposed estimator outperformed LS and
132 LMMSE estimators in terms of BER and MSE metrics.

133 In this study, a BiLSTM DLNN-based CSIE for OFDM wireless communication systems is
134 proposed and implemented. To the best of the authors' knowledge, this work is the first to use the
135 BiLSTM network as a CSIE without integration with CNN. The proposed estimator does not need
136 any prior knowledge of the communication channel statistics and powerfully works at limited
137 pilots (under the condition of less CSI). The proposed BiLSTM-based CSIE is a data-driven
138 estimator, so it can analyse, recognise and understand the statistical characteristics of wireless
139 channels suffering from many known interferences such as adjacent channel, inter symbol, inter
140 user, inter cell, co-channel and electromagnetic interferences and unknown ones (Jeya et al. 2019;
141 Sheikh 2004). Although an impressively wide range of configurations can be found for almost
142 every aspect of deep neural networks, the choice of loss function is underrepresented when
143 addressing communication problems, and most studies and applications simply use the 'log' loss
144 function (Janocha & Czarnecki 2017). In this study two customised loss functions known as mean

145 absolute error (MAE), and sum of squared errors (SSE) are proposed to obtain the most reliable
146 and robust estimator under unknown channel statistical characteristics and limited pilot numbers.

147 The performance of the proposed BiLSTM-based estimator is compared with the performance
148 of the most frequently used LS and MMSE channel state estimators. The obtained results show
149 that the BiLSTM-based estimator attains a comparable performance as the MMSE estimator and
150 outperforms LS and MMSE estimators at large and small numbers of pilots, respectively. In
151 addition, the proposed estimator improves the transmission data rate of OFDM wireless
152 communication systems because it exhibits optimal performance compared with the examined
153 estimators at a small number of pilots.

154 The rest of this paper is organised as follows. The DLNN-based CSIE is presented in Section
155 II. The standard OFDM system and the proposed deep learning BiLSTM NN-based CSIE are
156 presented in Section III. The simulation results are given in Section IV. The conclusions and future
157 work directions are provided in Section V.

158

159 DLNN-BASED CSIE

160 In this section, a deep learning BiLSTM NN for channel state information estimation is presented.
161 The BiLSTM network is another version of LSTM neural networks, which are recurrent neural
162 networks (RNN) that can learn the long-term dependencies between the time steps of input data
163 (Hochreiter & Schmidhuber 1997) (Luo et al. 2018b; Zhao et al. 2020).

164 The BiLSTM architecture mainly consists of two separate LSTM-NNs and has two propagation
165 directions (forward and backward). The LSTM NN structure consists of input, output and forget
166 gates and a memory cell. The forget and input gates enable the LSTM NN to effectively store long-
167 term memory. Figure 1 shows the main construction of the LSTM cell (Hochreiter & Schmidhuber
168 1997). The forget gate enables LSTM NN to remove the undesired information by currently used
169 input x_t and cell output h_t of the last process. The input gate finds the information that will be used
170 with the previous LSTM cell state c_{t-1} to obtain a new cell state c_t based on the current cell input
171 x_t and the previous cell output h_{t-1} . Using the forget and input gates, LSTM can decide which
172 information is abandoned and which is retained.

173 The output gate finds current cell output h_t by using the previous cell output h_{t-1} at current cell
174 state c_t and input x_t . The mathematical model of the LSTMNN structure can be described through
175 Equations (1) – (6).

$$176 \quad i_t = \sigma_g (w_i x_t + R_i h_{t-1} + b_i), \quad (1)$$

$$177 \quad f_t = \sigma_g (w_f x_t + R_f h_{t-1} + b_f), \quad (2)$$

$$178 \quad g_t = \sigma_c (w_g x_t + R_g h_{t-1} + b_g), \quad (3)$$

$$179 \quad o_t = \sigma_g (w_o x_t + R_o h_{t-1} + b_o), \quad (4)$$

$$180 \quad c_t = f_t \odot c_{t-1} + i_t \odot g_t, \quad (5)$$

$$181 \quad h_t = o_t \odot \sigma_c(c_t), \quad (6)$$

182 where $i, f, g, o, \sigma_c, \sigma_g$ and \odot denote the input gate, forget gate, cell candidate, output gate, state
183 activation function (hyperbolic tangent function (tanh), gate activation function (sigmoid function)
184 and Hadamard product (element-wise multiplication of vectors), respectively. $\mathbf{w} = [w_i \ w_f \ w_g \ w_o]^T$,
185 $\mathbf{R} = [R_i \ R_f \ R_g \ R_o]^T$ and $\mathbf{b} = [b_i \ b_f \ b_g \ b_o]^T$ are input weights, recurrent weights and bias, respectively.

186 LSTM DNN, only analyses the impact of the previous sequence in the present, disregarding
187 information later on and failing to reach optimal performance. On the other hand BiLSTM
188 connects the LSTM unit's output bidirectionally (forward and backward propagation directions)
189 and capture bidirectional signals dependencies, increasing the overall model's performance.

190 The forward and backward propagation directions of BiLSTM are transmitted at the same time
191 to the output unit. Therefore, old and future information can be captured, as shown in Figure 2. At

192 any time t , the input is fed to forward LSTM and backward LSTM networks. The final output of
193 BiLSTM-NN can be expressed as follows:

$$194 \quad h_t = \vec{h}_t \odot \overleftarrow{h}_t, \quad (7)$$

195 where \vec{h}_t and \overleftarrow{h}_t are forward and backward outputs of BiLSTM-NN, respectively. The operation of
196 BiLSTM in the proposed estimator can be described briefly by the following algorithm:

197
198 Input: sequence represents transmitted signal (original signal + channel model)

199 Output: Prediction matrix of the extracted features of the input sequence

200 Step 1: The forward LSTM layer receives the transmitted signal vectors from X .

201 for $i \in \text{length}(X)$ do

202 send X_i to BiLSTM Layer

203 end for

204 Step 2: Equations 1–6 are used to update the state of the LSTM cell.

205 Step 3: The backward LSTM layer receives the signal vectors from X , and the two previous steps
206 are repeated.

207 Step 4: A hidden state sequence vector is created by splicing the forward and backward sequences
208 of hidden layers.

209 Step 5: A hidden state sequence vector is sent into a full connection layer and the prediction matrix
210 is obtained

211 Step 6: Return the prediction matrix.

212

213 To build the DL BiLSTM NN-based CSIE, an array is created with the following five layers:
214 sequence input, BiLSTM, fully connected, softmax and output classification. The input size was
215 set to 256. The BiLSTM layer consists of 30 hidden units and shows the sequence's last element.
216 Four classes are specified by considering the size 4 fully connected (FC) layer, followed by a
217 softmax layer and ended by a classification layer. Figure 3 illustrates the structure of the proposed
218 estimator (Essai Ali ; Ye et al. 2018).

219 As the proposed BiLSTM-based CSIE is built, the weights and biases of the proposed estimator
220 are optimised (tuned) using the desired optimisation algorithm. The optimisation algorithm trains
221 the proposed estimator by using one of three loss functions, namely, cross entropy function for k^{th}
222 mutually exclusive classes (crossentropyex), mean absolute error (MAE), and sum of squared
223 errors (SSE). The loss function estimates the loss between the expected and actual outcome.
224 During the learning process, optimisation algorithms try to minimise the available loss function to
225 the desired error goal by optimising the DLNN weights and biases iteratively at each training
226 epoch. Figure 4 illustrates the training processes of the proposed estimator. Selecting a loss
227 function is one of the essential and challenging tasks in deep learning. Also, investigating the
228 efficiency of the training process using different optimization algorithms such as Adaptive
229 Moment Estimation (Adam), Root Mean Square Propagation (RMSProp), Stochastic Gradient
230 Descent with momentum (SGdm) (Dogo et al. 2018), and an adaptive learning rate method
231 (Adadelata) (Zeiler 2012). The proposed estimator is trained using above-mentioned three different
232 loss functions and optimization algorithms to obtain the most optimal BiLSTM-based estimator
233 for wireless communication systems with low prior information (limited pilots) for signal-noise
234 environments.

235

236

237 **DL BiLSTM NN-BASED CSIE for 5G-OFDM WIRELESS** 238 **COMMUNICATION SYSTEMS**

239 The standard OFDM wireless communication system and an offline DL of the proposed CSIE are
240 presented in the following subsections.

241

242 **OFDM SYSTEM MODEL**

243 In accordance with (Essai Ali ; Ye et al. 2018), Figure 5 clearly illustrates the structure of the
244 traditional OFDM communication system. On the transmitter side, a serial-to-parallel (S/P)
245 converter is used to convert the transmitted symbols with pilot signals into parallel data streams.
246 Then, inverse discrete Fourier transform (IDFT) is applied to convert the signal into the time
247 domain. A cyclic prefix (CP) must be added to alleviate the effects of inter-symbol interference.
248 The length of the CP must be longer than the maximum spreading delay of the channel.

249 The multipath channel of a sample space defined by complex random variables $\{h(n)\}_{n=0}^{N-1}$ is
250 considered. Then, the received signal can be evaluated as follows:

$$251 \quad y(n) = x(n) \oplus h(n) + w(n), \quad (8)$$

252 where $x(n)$ is the input signal, \oplus is circular convolution, $w(n)$ is additive white Gaussian noise
253 (AWGN) and $y(n)$ is the output signal.

254 The received signal in the frequency domain can be defined as

$$255 \quad Y(k) = X(k)H(k) + W(k), \quad (9)$$

256 where the discrete Fourier transformations (DFT) of $x(n)$, $h(n)$, $y(n)$ and $w(n)$ are $X(k)$, $H(k)$,
257 $Y(k)$ and $W(k)$, respectively. These discrete Fourier transformations are estimated after removing
258 CP.

259 The OFDM frame includes the pilot symbols of the 1st OFDM block and the transmitted data of
260 the next OFDM blocks. The channel can be considered stationary during a certain frame, but it can
261 change between different frames. The proposed DL BiLSTM NN-based CSIE receives the arrived
262 data at its input terminal and extracts the transmitted data at its output terminal (Essai Ali), (Ye et al.
263 2018).

264

265 **OFFLINE DL OF THE DL BILSTM NN-BASED CSIE**

266 DLNN utilisation is the state-of-the-art approach in the field of wireless communication, but
267 DLNNs have high computational complexity and long training time. GPUs are the most powerful
268 tools used for training DLNNs (Sharma et al. 2016). Training should be done offline due to the
269 long training time of the proposed CSIE and the large number of BILSTM-NN's parameters, such
270 as biases and weights, that should be tuned during training. The trained CSIE is then used in online
271 implementation to extract the transmitted data (Ye et al. 2018), (Essai Ali).

272 In offline training, the learning dataset is randomly generated for one subcarrier. The
273 transmitting end sends OFDM frames to the receiving end through the adopted (simulated)
274 channel, where each frame consists of single OFDM pilot symbol and a single OFDM data symbol.
275 The received OFDM signal is extracted based on OFDM frames that are subjected to different
276 channel imperfections.

277 All classical estimators rely highly on tractable mathematical channel models, which are
278 assumed to be linear, stationary and follow Gaussian statistics. However, practical wireless
279 communication systems have other imperfections and unknown surrounding effects that cannot be
280 tackled well by accurate channel models; therefore, researchers have developed various channel
281 models that effectively characterise practical channel statistics. By using these channel models,
282 reliable and practical training datasets can be obtained by modelling (Bogdanovich et al. 2009),
283 (Essai Ali), (2019).

284 In this study, the 3GPP TR38.901-5G channel model developed by (2019) is used to simulate
285 the behaviour of a practical wireless channel that can degrade the performance of CSIEs and hence,
286 the overall communication system's performance.

287 The proposed estimator is trained via the algorithm, which updates the weights and biases by
288 minimising a specific loss function. Simply, a loss function is defined as the difference between

289 the estimator's responses and the original transmitted data. The loss function can be represented
 290 by several functions. MATLAB/neural network toolbox allows the user to choose a loss function
 291 amongst its available list that contains crossentropyex, MSE, sigmoid and softmax. In this study,
 292 another two custom loss functions (MAE and SSE) are created. The performance of the proposed
 293 estimator when using three loss functions (i.e. MAE, crossentropyex and SSE) is investigated. The
 294 loss functions can be expressed as follows:

$$295 \quad \text{crossentropyex} = -\sum_{i=1}^N \sum_{j=1}^c X_{ij}(k) \log(\hat{X}_{ij}(k)), \quad (10)$$

$$296 \quad \text{MAE} = \frac{\sum_{i=1}^N \sum_{j=1}^c |X_{ij}(k) - \hat{X}_{ij}(k)|}{N}, \quad (11)$$

$$297 \quad \text{SSE} = \sum_{i=1}^N \sum_{j=1}^c (X_{ij}(k) - \hat{X}_{ij}(k))^2, \quad (12)$$

298

299 where N is the sample number, c is the class number, X_{ij} is the i^{th} transmitted data sample for the
 300 j^{th} class and \hat{X}_{ij} is the DL BiLSTM-based CSIE response for sample i for class j .

301 Figure 4 illustrates the offline training processes to obtain a learned CSIE based on BiLSTM-
 302 NN.

303

304 Simulation Results

305 STUDYING THE PERFORMANCE OF THE PROPOSED, LS AND MMSE 306 ESTIMATORS BY USING DIFFERENT PILOTS AND LOSS FUNCTIONS

307 Several simulation experiments are performed to evaluate the performance of the proposed
 308 estimator. In terms of symbol error rate (SER) performance analysis, the SER performance of the
 309 proposed estimator under various SNRs is compared with that of the LSTM NN-based CSIE (Essai
 310 Ali), the well-known LS estimator and the MMSE estimator, which is an optimal estimator but
 311 requires channel statistical information. A priori uncertainty of the used channel model statistics is
 312 assumed and considered for all conducted experiments.

313 Moreover, the Adam optimisation algorithm is used to train the proposed estimator whilst using
 314 different loss functions to obtain the most robust version of the proposed CSIE. The proposed model
 315 is implemented in 2019b MATLAB/software.

316 Table 1 lists the parameters of BiLSTM-NN and LSTM-NN architectures and their related training
 317 options. These parameters are identified by a trial-and-error approach. Table 2 lists the parameters
 318 of the OFDM system model and the channel model.

319 The examined estimators' performance is evaluated at different pilot numbers of 4, 8 and 64 as
 320 well as crossentropyex, MAE and SSE loss functions. The Adam optimisation algorithm is used for
 321 all simulation experiments.

322 With a sufficiently large number of pilots (64) and the use of the crossentropyex loss function, the
 323 proposed BiLSTM_{crossentropyex} estimator outperforms LSTM_{crossentropyex}, LS and MMSE estimators
 324 over the entire SNR range, as shown in Figure 6. At the use of the MAE loss function, the
 325 BiLSTM_{MAE} estimator outperforms the LS estimator over the SNR range [0–18 dB], but LSTM_{MAE}
 326 outperforms it over the SNR range [0–14 dB]. In addition, the BiLSTM_{MAE} and LSTM_{MAE} estimators
 327 are at par with the MMSE estimator over the SNR ranges [0–10 dB] and [0–4 dB], respectively.
 328 Beyond these SNR ranges, the MMSE estimator outperforms BiLSTM_{MAE} and LSTM_{MAE}
 329 estimators. BiLSTM_{MAE} outperforms LSTM_{MAE} starting from 0 dB to 20 dB.

330 At the use of the SSE loss function, Figure 6 shows that the BiLSTM_{SSE} and LSTM_{SSE} estimators
 331 achieve approximately the same performance as the MMSE estimator over a low SNR range [0–6
 332 dB]. MMSE outperforms the BiLSTM_{SSE} and LSTM_{SSE} estimators starting from 8 dB, and the LS
 333 estimator outperforms BiLSTM_{SSE} starting from 16 dB and LSTM_{SSE} starting from 14 dB.
 334 BiLSTM_{SSE} outperforms LSTM_{SSE} starting from 10 dB to 20 dB. LS provides poor performance
 335 compared with MMSE because it does not use prior information about channel statistics in the

336 estimation process. MMSE exhibits superior performance, especially with sufficient pilot numbers,
337 because it uses second-order channel statistics. Concisely, MMSE and the proposed
338 $\text{BiLSTM}_{\text{crossentropyex}}$ attain close SER performance with respect to all SNRs. Furthermore, at low SNR
339 (0–6 dB), $\text{BiLSTM}_{\text{(crossentropyex, MAE, and SSE)}}$, $\text{LSTM}_{\text{(crossentropyex, MAE, and SSE)}}$ and MMSE attain
340 approximately the same performance.

341 Figures 7 present the performance comparison of LS, MMSE, BiLSTM and LSTM-based
342 estimators using the Adam optimisation algorithm and the different (crossentropyex, MAE and SSE)
343 loss functions at 8 pilots. Figure 7 shows that the proposed $\text{BiLSTM}_{\text{(crossentropyex, or MAE or SSE)}}$ estimators
344 outperform the $\text{LSTM}_{\text{(crossentropyex, or MAE or SSE)}}$ estimators and the traditional estimators over the
345 examined SNR range. At a low SNR (0–7 dB), the proposed $\text{BiLSTM}_{\text{(crossentropyex, or MAE or SSE)}}$
346 estimators exhibit semi-identical performance. Furthermore, the proposed $\text{BiLSTM}_{\text{SSE}}$ estimator
347 trained by minimising the SSE loss function outperforms the $\text{BiLSTM}_{\text{crossentropyex}}$ estimator trained
348 by minimising the crossentropyex loss function starting from 0 dB; also it outperforms $\text{BiLSTM}_{\text{MAE}}$,
349 which is trained by minimising the MAE loss function starting from 14 dB. Concisely at 8 pilots
350 $\text{BiLSTM}_{\text{SSE}}$ estimator achieved the most minimum SER.

351 Figures 8 show the performance comparison of the LS, MMSE, $\text{BiLSTM}_{\text{(crossentropyex, or MAE or SSE)}}$
352 and $\text{LSTM}_{\text{(crossentropyex, or MAE or SSE)}}$ estimators at 4 pilots. Figure 8 shows the superiority of the
353 proposed $\text{BiLSTM}_{\text{(crossentropyex, or MAE or SSE)}}$ estimators in comparison with the traditional estimators,
354 which have lost their workability starting from 0 dB. It also shows the superiority of the proposed
355 estimator $\text{BiLSTM}_{\text{(MAE or SSE)}}$ over $\text{LSTM}_{\text{(MAE or SSE)}}$. $\text{LSTM}_{\text{(crossentropyex)}}$ exhibits a competitive
356 performance as $\text{BiLSTM}_{\text{(crossentropyex)}}$ starting from 0 dB to 12 dB, and $\text{LSTM}_{\text{(crossentropyex)}}$
357 outperforms $\text{BiLSTM}_{\text{(crossentropyex)}}$ starting from 14 dB. At very low SNRs (0–3 dB), the proposed
358 $\text{BiLSTM}_{\text{(crossentropyex, or MAE or SSE)}}$ estimators have the same performance. The proposed $\text{BiLSTM}_{\text{SSE}}$
359 estimator outperforms the $\text{BiLSTM}_{\text{crossentropyex}}$ estimator starting from 4 dB, and it exhibits an
360 identical performance as the $\text{BiLSTM}_{\text{MAE}}$ estimator until 14 dB and outperforms it in the rest of
361 the SNR examination range.

362 Figures 6, 7 and 8 emphasise the robustness of the BiLSTM-based estimators against the limited
363 number of pilots, low SNR, and under the condition of a priori uncertainty of channel statistics.
364 They demonstrate the importance of testing various loss functions in the deep learning process to
365 obtain the most optimal architecture of any proposed estimator.

366 Figure 9 indicates that the proposed $\text{BiLSTM}_{\text{crossentropyex}}$, $\text{BiLSTM}_{\text{SSE}}$ and $\text{BiLSTM}_{\text{SSE}}$ estimators
367 have close SER performance at 64, 8 and 4 pilots, respectively. The performance of $\text{BiLSTM}_{\text{SSE}}$
368 at 8 pilots coincides with the performance of $\text{BiLSTM}_{\text{crossentropyex}}$ at 64 pilots. Therefore, using the
369 proposed estimators with few pilots is recommended for 5G OFDM wireless communication
370 systems to attain a significant improvement in their transmission data rate. Given that the proposed
371 estimator adopts a training data set-driven approach, it is robust to a priori uncertainty for channel
372 statistics.

373

374

375 LOSS CURVES

376 The quality of the DLNNs' training process can be monitored efficiently by exploring the
377 training loss curves. These loss curves provide information on how the training process goes, and
378 the user can decide whether to let the training process continue or stop.

379 Figures 10–12 show the loss curves of the DLNN-based estimators (BiLSTM and LSTM) at
380 pilot numbers = 64, 8 and 4 and with the three examined loss functions (crossentropyex, MAE and
381 SSE). The curves emphasise and verify the obtained results in Figure 6, 7, and 8. For example, the
382 sub-curves in Figure 10 for $\text{BiLSTM}_{\text{crossentropyex}}$ and $\text{LSTM}_{\text{crossentropyex}}$ estimators emphasise their
383 superiority over the other estimators. This superiority can be seen clearly from Figures 6.
384 Moreover, the training loss curves in Figures 11 and 12 emphasise the obtained SER performance
385 in Figures 7 and 8, respectively, of each examined DLNN-based CSIE. For more details, good
386 zooming, and analysis of the presented loss curves, they can be downloaded from this link
387 (shorturl.at/lqxGQ).

388

389 ACCURACY CALCULATION

390 The accuracy of the proposed and other examined estimators is a measure of how the estimators
391 recover transmitted data correctly. Accuracy can be defined as the number of correctly received
392 symbols divided by the total number of transmitted symbols. The proposed estimator is trained in
393 different conditions as indicated in the previous subsection, and we wish to investigate how well
394 it performs in a new data set. Tables 3, 4 and 5 present the obtained accuracies for all examined
395 estimators under all simulation conditions.

396 As illustrated in Tables 3 to 5, the proposed BiLSTM-based estimator attains accuracies from
397 98.61 to 100 under different pilots and loss functions. The other examined DL LSTM-based
398 estimator has accuracies from 97.88 to 99.99 under the same examination conditions. The achieved
399 accuracies indicate that the proposed estimator has robustly learned and emphasises the obtained
400 SER performance in Figure 9. The obtained results of MMSE and LS in Tables 1, 2 and 3
401 emphasise the presented SER performance in Figures 6, 7 and 8, respectively, and show that as
402 the pilot number decreases, the accuracy of the conventional estimators dramatically decreases.

403 The proposed BiLSTM- and LSTM-based estimators rely on DLNN approaches, where they can
404 analyse huge data sets that may be collected from any plant, recognise the statistical dependencies
405 and characteristics, devise the relationships between features and generalise the accrued
406 knowledge for new data sets that they have not seen before. Thus, they are applicable to any 5G
407 and beyond communication system.

408

409 IMPACT OF USING DIFFERENT OPTIMIZATION ALGORITHMS ON THE 410 PROPOSED ESTMATOR PERFORMANCE

411 DL procedures benefit greatly from optimization methods. DNN training can be thought of as an
412 optimisation issue that aims to discover a global optimum by applying gradient descent methods to
413 obtain a robust training, and hence reliable prediction or classification models. Choosing the best
414 optimization method for a particular scientific topic is a difficult task. Using the wrong optimization
415 strategy during training can cause the DN to stay at the local minimum, which results in no training
416 progress (Dogo et al. 2018). As a result, examination is required to evaluate the performance of
417 various optimisers to get the optimal CSIE.

418 This section provides performance comparison experiments using RMSProp, SGdm, and
419 Adadelta optimisation algorithms (Soydaneer & Intelligence 2020) for training the proposed
420 BiLSTM-based CSIE at using 8-pilots, as illustrated in Fig.13. Table 6 arranges the proposed
421 BiLSTM CSIE estimators using different optimisation algorithms and loss functions from the
422 highest performance to the lowest and their related accuracies.

423 It is clear from Fig.13 and Table 6 that the trained BiLSTM-based CSIE using Adadelta
424 optimisation algorithm and SSE loss function achieves the best SER performance and provides the
425 highest accuracy with 100%. On the other hand, the same estimator achieves the lowest SER
426 performance and provides accuracy with 97.46% using SGdm optimization algorithm and SSE loss
427 function. This, in turn, shows the importance of studying the training process efficiency using
428 different optimization algorithms in the case of using a specific loss function.

429

430

431 CONCLUSIONS and FUTURE WORK

432 The proposed DL-BiLSTM-based CSIE is an online pilot-assisted estimator. It is robust against a
433 limited number of pilots and exhibits superior performance compared with conventional estimators;
434 it is also robust under the conditions of a priori uncertainty of communication channel statistics
435 (non-Gaussian/stationary statistical channels) and demonstrates superior performance compared
436 with conventional estimators and DL LSTM NN-based CSIEs.

437 Two customized classification layers using the loss functions (MAE and SSE) are introduced. The
438 proposed CSIE exhibits a consistent performance at large and small pilot numbers and superior
439 performance at low SNRs, especially at limited pilots, compared with conventional estimators. It

440 also achieves the highest accuracy amongst all examined estimators at 64, 8, and 4 pilots for all
441 the used loss functions.

442 The proposed BiLSTM- and LSTM-based estimators have high prediction accuracies of 98.61%
443 to 100% and 97.88% to 99.99%, respectively, when using crossentropyex, MAE, and SSE loss
444 functions for 64, 8, and 4 pilots. The proposed BiLSTM using (Adam, and crossentropyex),
445 BiLSTM using (Adam, MAE, and SSE; and Adadelata, and SSE), and BiLSTM using (Adam, and
446 SSE), achieve the best SER performance and provide accuracies with 100% at 64, 8, and 4 pilots
447 respectively. The proposed estimator is promising for 5G and beyond wireless communication
448 systems.

449 For future work, authors suggest the following research plans:

- 450 1. Investigating the proposed estimator's performance and accuracy by using different cyclic prefix
451 lengths and types.
- 452 2. Developing robust loss functions by using robust statistics estimators, such as Tukey, Cauchy,
453 Huber and Welsh.
- 454 3. Investigating the performance of CNN-, gated recurrent unit (GRU)- and simple recurrent unit
455 (SRU)-based CSIEs whilst using crossentropyex, MAE and SSE loss functions and for 64, 8 and
456 4 pilots.

457

458 Acknowledgements

459 The authors would like to acknowledge the financial support received from Taif University
460 Researchers Supporting Project Number (TURSP-2020/61), Taif University, Taif, Saudi Arabia.

461

462 References

- 463 2019. 3GPP. TR38.901 Study on Channel Model for Frequencies from 0.5 to 100 GHz; 3GPP:
464 Sophia Antipolis, France, 2019.
- 465 Bogdanovich V, Vostretsov AJJoCT, and Electronics. 2009. Application of the invariance and
466 robustness principles in the development of demodulation algorithms for wideband
467 communications systems. 54:1283-1291.
- 468 Dogo E, Afolabi O, Nwulu N, Twala B, and Aigbavboa C. 2018. A comparative analysis of
469 gradient descent-based optimization algorithms on convolutional neural networks. 2018
470 International Conference on Computational Techniques, Electronics and Mechanical
471 Systems (CTEMS): IEEE. p 92-99.
- 472 Essai Ali MH. Deep learning-based pilot-assisted channel state estimator for OFDM systems. *IET*
473 *Communications* 15:257-264. <https://doi.org/10.1049/cmu2.12051>
- 474 Hochreiter S, and Schmidhuber J. 1997. Long Short-Term Memory. 9:1735-1780.
475 10.1162/neco.1997.9.8.1735
- 476 Janocha K, and Czarnecki WMJapa. 2017. On loss functions for deep neural networks in
477 classification.
- 478 Jeya R, Amutha B, Nikhilesh N, and Immaculate RRJs. 2019. Signal Interferences in Wireless
479 Communication-An Overview. 2:3.
- 480 Joo J, Park MC, Han DS, and Pejovic VJIA. 2019. Deep learning-based channel prediction in
481 realistic vehicular communications. *IEEE Access* 7:27846-27858.
- 482 Kang J-M, Chun C-J, and Kim I-MJIA. 2020. Deep Learning Based Channel Estimation for
483 MIMO Systems With Received SNR Feedback. *IEEE Access* 8:121162-121181.
- 484 Karra K, Kuzdeba S, and Petersen J. 2017. Modulation recognition using hierarchical deep neural
485 networks. 2017 IEEE International Symposium on Dynamic Spectrum Access Networks
486 (DySPAN). p 1-3.

- 487 Kim H. 2015. *Wireless communications systems design*: John Wiley & Sons.
- 488 Le Ha A, Van Chien T, Nguyen TH, and Choi W. 2021. Deep Learning-Aided 5G Channel
489 Estimation. 2021 15th International Conference on Ubiquitous Information Management
490 and Communication (IMCOM): IEEE. p 1-7.
- 491 Liao Y, Hua Y, Dai X, Yao H, and Yang X. 2019. ChanEstNet: A deep learning based channel
492 estimation for high-speed scenarios. ICC 2019-2019 IEEE International Conference on
493 Communications (ICC): IEEE. p 1-6.
- 494 Luo C, Ji J, Wang Q, Chen X, Li PJIToNS, and Engineering. 2018a. Channel state information
495 prediction for 5G wireless communications: A deep learning approach. 7:227-236.
- 496 Luo C, Ji J, Wang Q, Chen X, Li PJIToNS, and Engineering. 2018b. Channel state information
497 prediction for 5G wireless communications: A deep learning approach.
- 498 Ma X, Ye H, and Li Y. 2018. Learning Assisted Estimation for Time- Varying Channels. 2018
499 15th International Symposium on Wireless Communication Systems (ISWCS). p 1-5.
- 500 O'Shea T, Karra K, and Clancy TC. 2017. Learning approximate neural estimators for wireless
501 channel state information. 2017 IEEE 27th international workshop on machine learning for
502 signal processing (MLSP): IEEE. p 1-7.
- 503 Ong T. 2017. Facebook's translations are now powered completely by AI.
- 504 Oyerinde OO, and Mneney SH. 2012a. Review of Channel Estimation for Wireless
505 Communication Systems. *IETE Technical Review* 29:282-298. 10.4103/0256-
506 4602.101308
- 507 Oyerinde OO, and Mneney SHJITr. 2012b. Review of channel estimation for wireless
508 communication systems. *IETE Technical Review* 29:282-298.
- 509 Ponnaluru S, and Penke S. 2020. Deep learning for estimating the channel in orthogonal frequency
510 division multiplexing systems. *Journal of Ambient Intelligence and Humanized*
511 *Computing*. 10.1007/s12652-020-02010-1
- 512 Sarwar A, Shah SM, and Zafar I. 2020. Channel Estimation in Space Time Block Coded MIMO-
513 OFDM System using Genetically Evolved Artificial Neural Network. 2020 17th
514 International Bhurban Conference on Applied Sciences and Technology (IBCAST): IEEE.
515 p 703-709.
- 516 Senol H, Tahir ARB, and Özmen AJTS. 2021. Artificial neural network based estimation of sparse
517 multipath channels in OFDM systems. *Telecommunication Systems*:1-10.
- 518 Sharma R, Vinutha M, and Moharir M. 2016. Revolutionizing machine learning algorithms using
519 gpus. 2016 International Conference on Computation System and Information Technology
520 for Sustainable Solutions (CSITSS): IEEE. p 318-323.
- 521 Sheikh AUH. 2004. Interference, Distortion and Noise. *Wireless Communications: Theory and*
522 *Techniques*. Boston, MA: Springer US, 225-285.
- 523 Soydaner DJIJoPR, and Intelligence A. 2020. A comparison of optimization algorithms for deep
524 learning. 34:2052013.
- 525 Wu Y, Schuster M, Chen Z, Le QV, Norouzi M, Macherey W, Krikun M, Cao Y, Gao Q, and
526 Macherey KJapa. 2016. Google's neural machine translation system: Bridging the gap
527 between human and machine translation.
- 528 Yang Y, Gao F, Ma X, and Zhang S. 2019a. Deep Learning-Based Channel Estimation for Doubly
529 Selective Fading Channels. *IEEE Access* 7:36579-36589.
530 10.1109/ACCESS.2019.2901066
- 531 Yang Y, Gao F, Ma X, and Zhang SJIA. 2019b. Deep learning-based channel estimation for doubly
532 selective fading channels. 7:36579-36589.

- 533 Ye H, Li GY, and Juang B. 2018. Power of Deep Learning for Channel Estimation and Signal
534 Detection in OFDM Systems. *IEEE Wireless Communications Letters* 7:114-117.
535 10.1109/LWC.2017.2757490
- 536 Zeiler MDJapa. 2012. Adadelata: an adaptive learning rate method.
- 537 Zhao C, Huang X, Li Y, and Yousaf Iqbal MJS. 2020. A Double-Channel Hybrid Deep Neural
538 Network Based on CNN and BiLSTM for Remaining Useful Life Prediction. 20:7109.
- 539 Zhou R, Liu F, and Gravelle CW. 2020. Deep Learning for Modulation Recognition: A Survey
540 With a Demonstration. *IEEE Access* 8:67366-67376. 10.1109/ACCESS.2020.2986330
541

Figure 1

Long short-term memory (LSTM) cell.

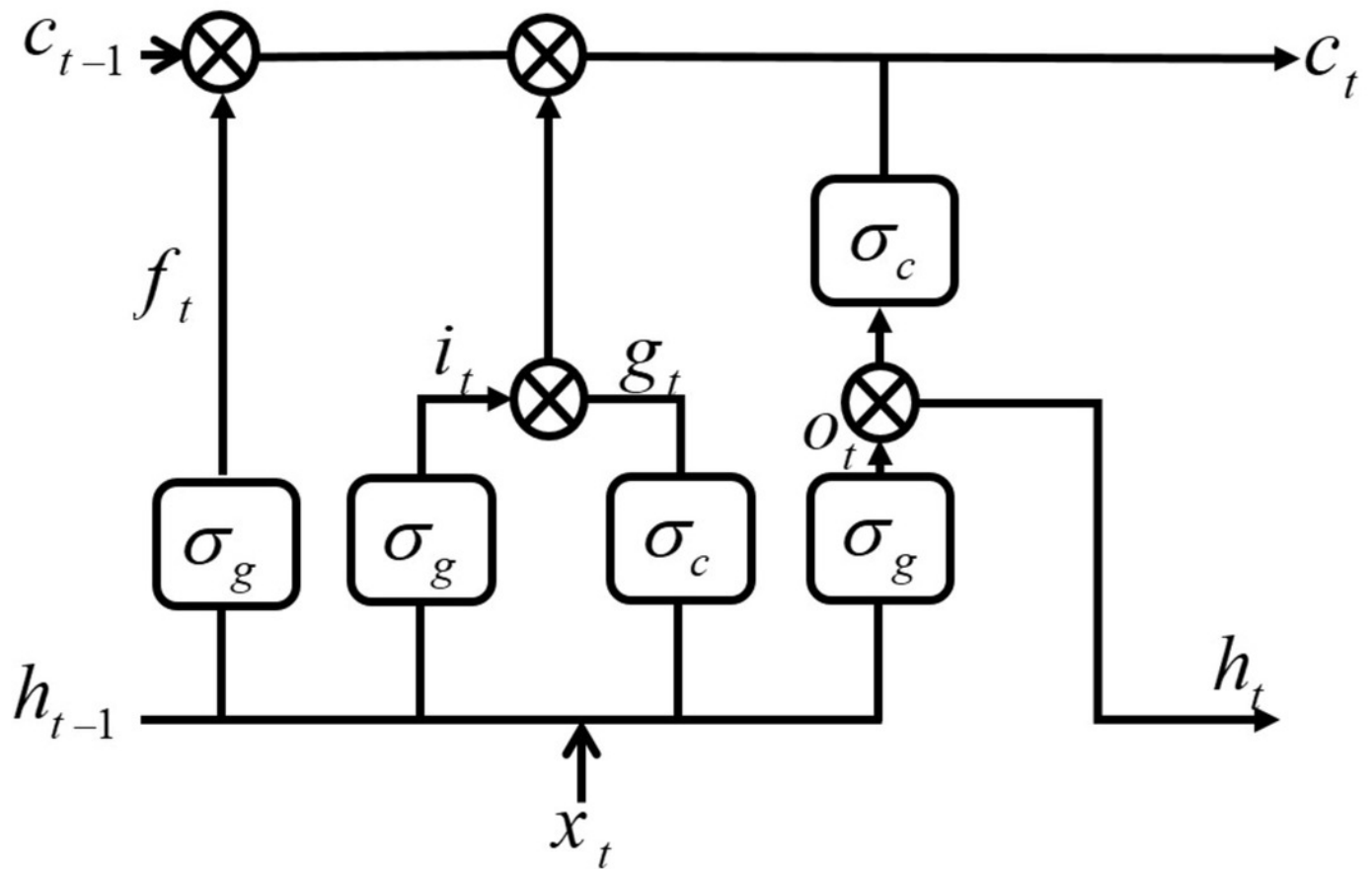


Figure 2

BiLSTM-NN architecture.

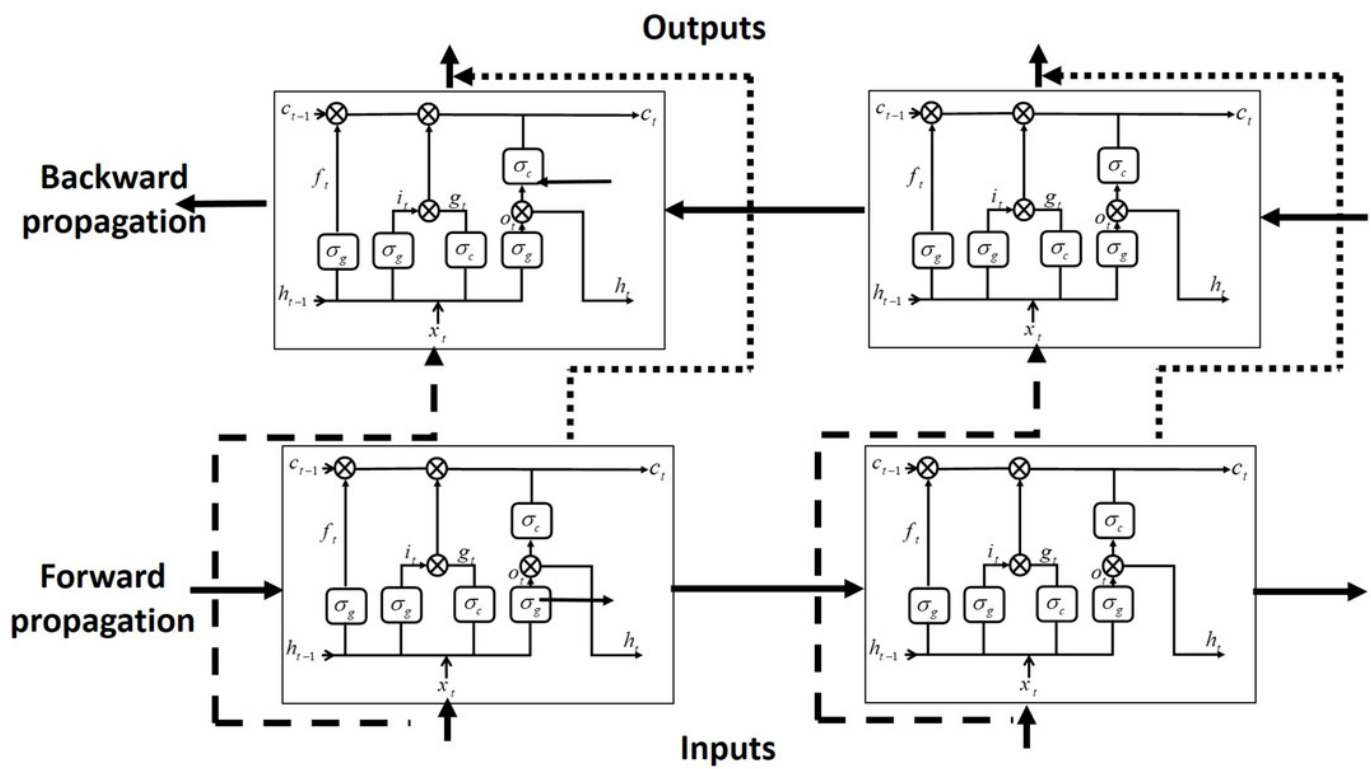


Figure 3

Structure of the DL BiLSTM NN for the BiLSTM estimator.

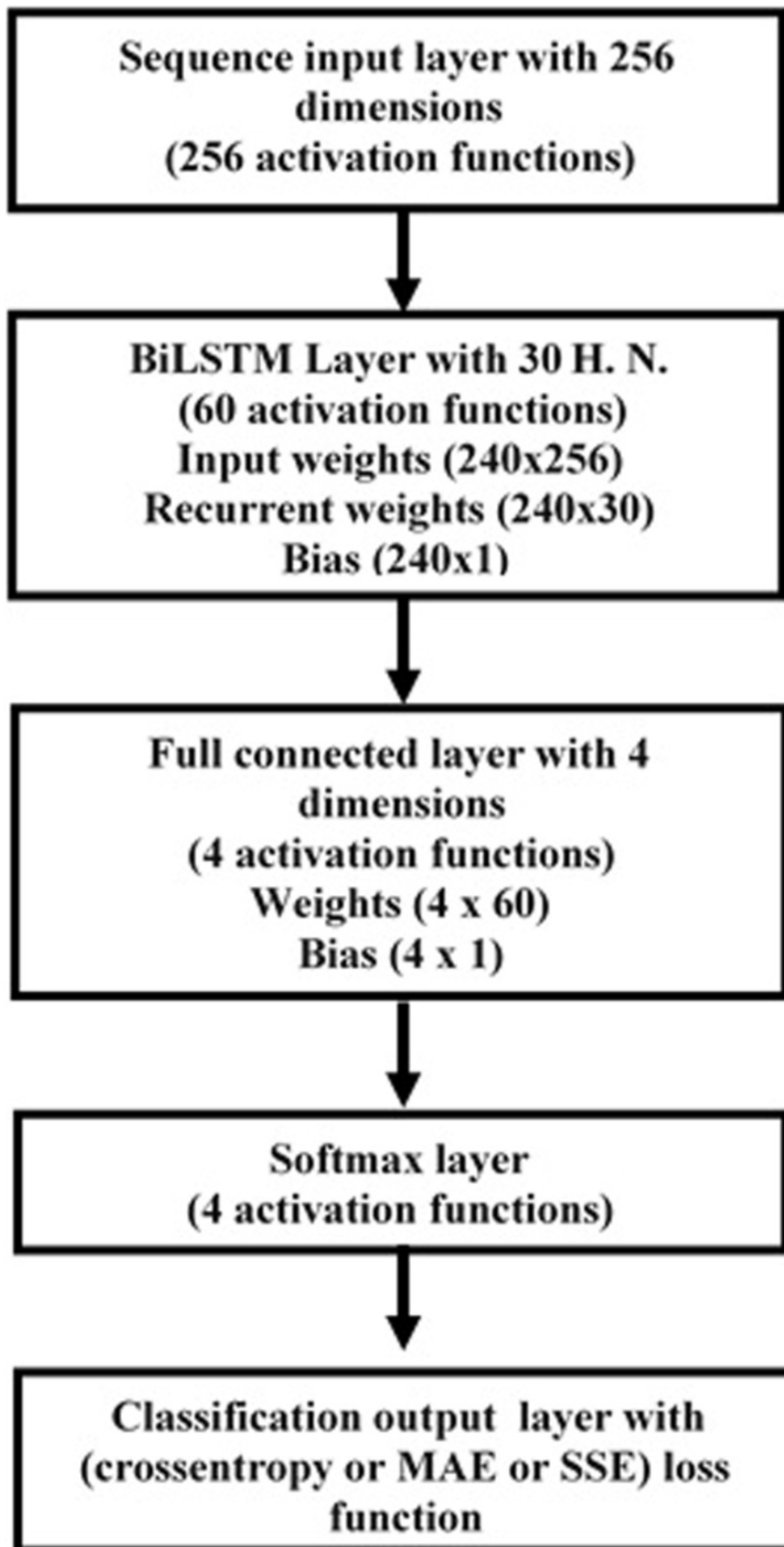


Figure 4

Offline training of the BiLSTM-NN-based CSI estimator.

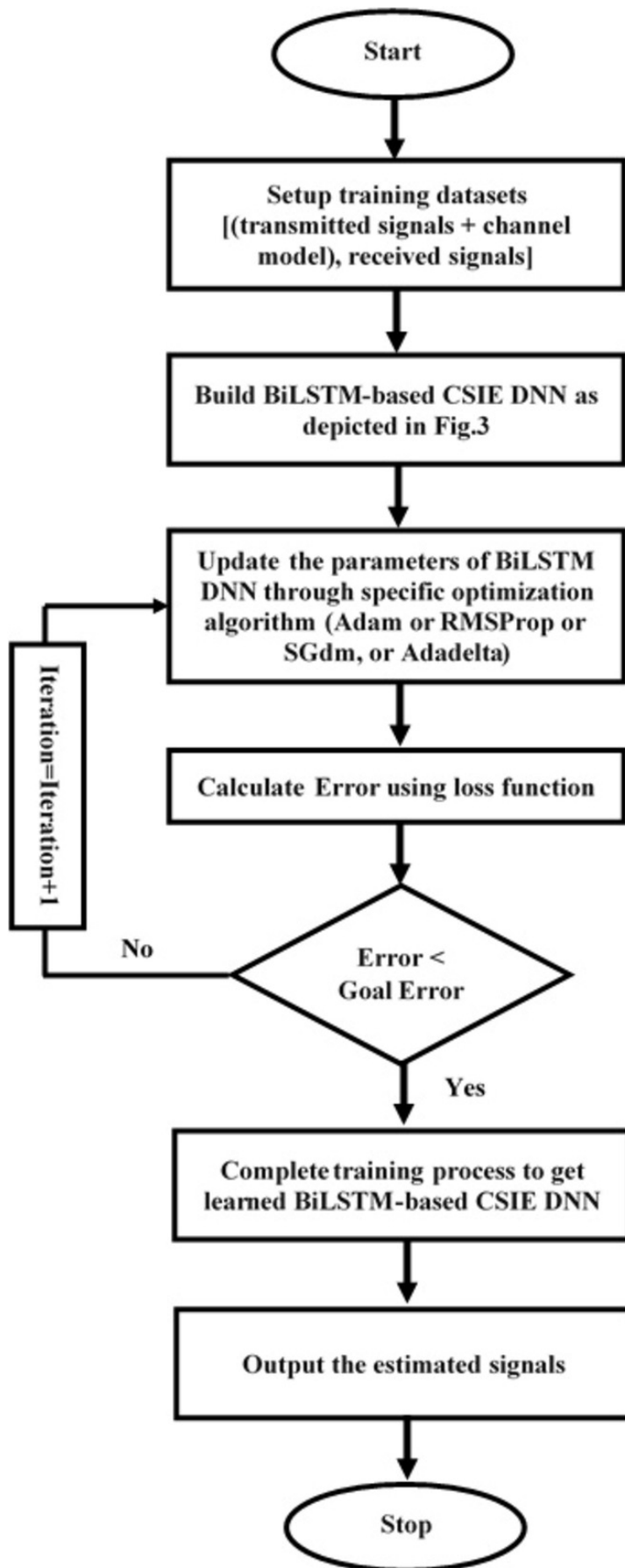


Figure 5

Conventional OFDM system

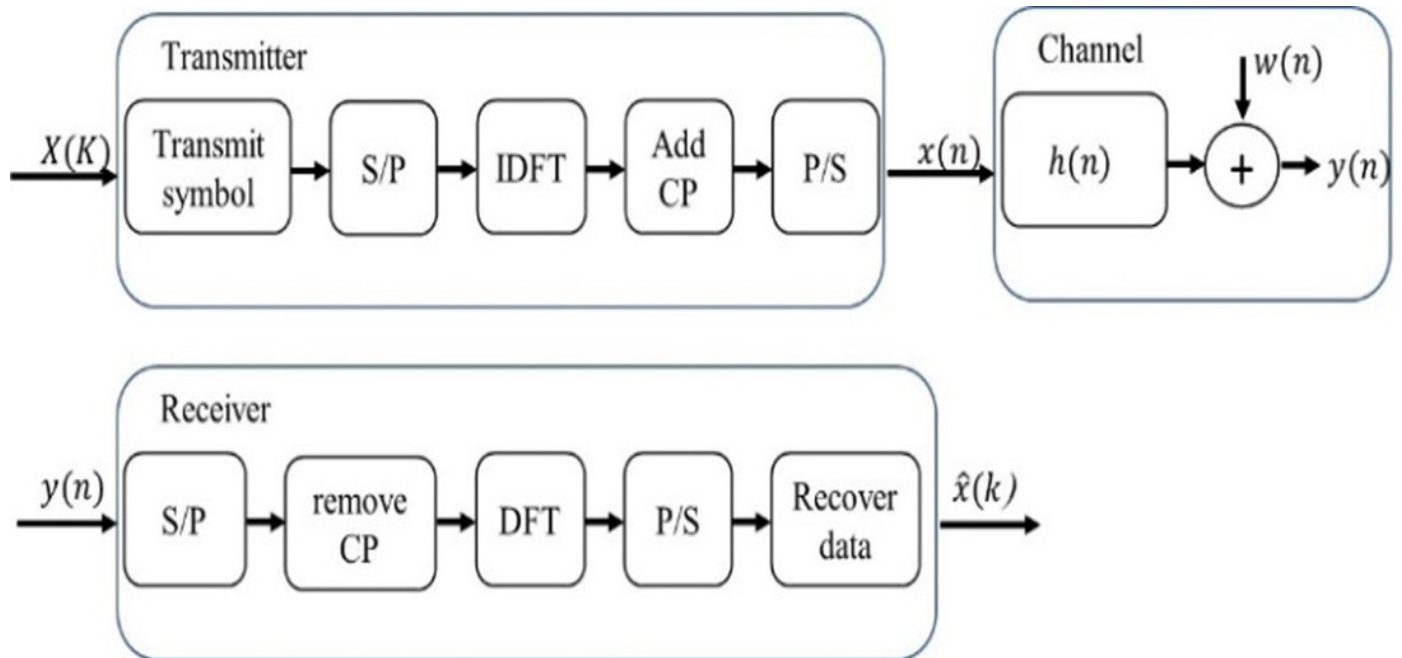


Figure 6

SER comparison of LS, MMSE, BiLSTM and LSTM estimators using 64 pilots, the Adam learning algorithm and crossentropyex, MAE and SSE loss functions.

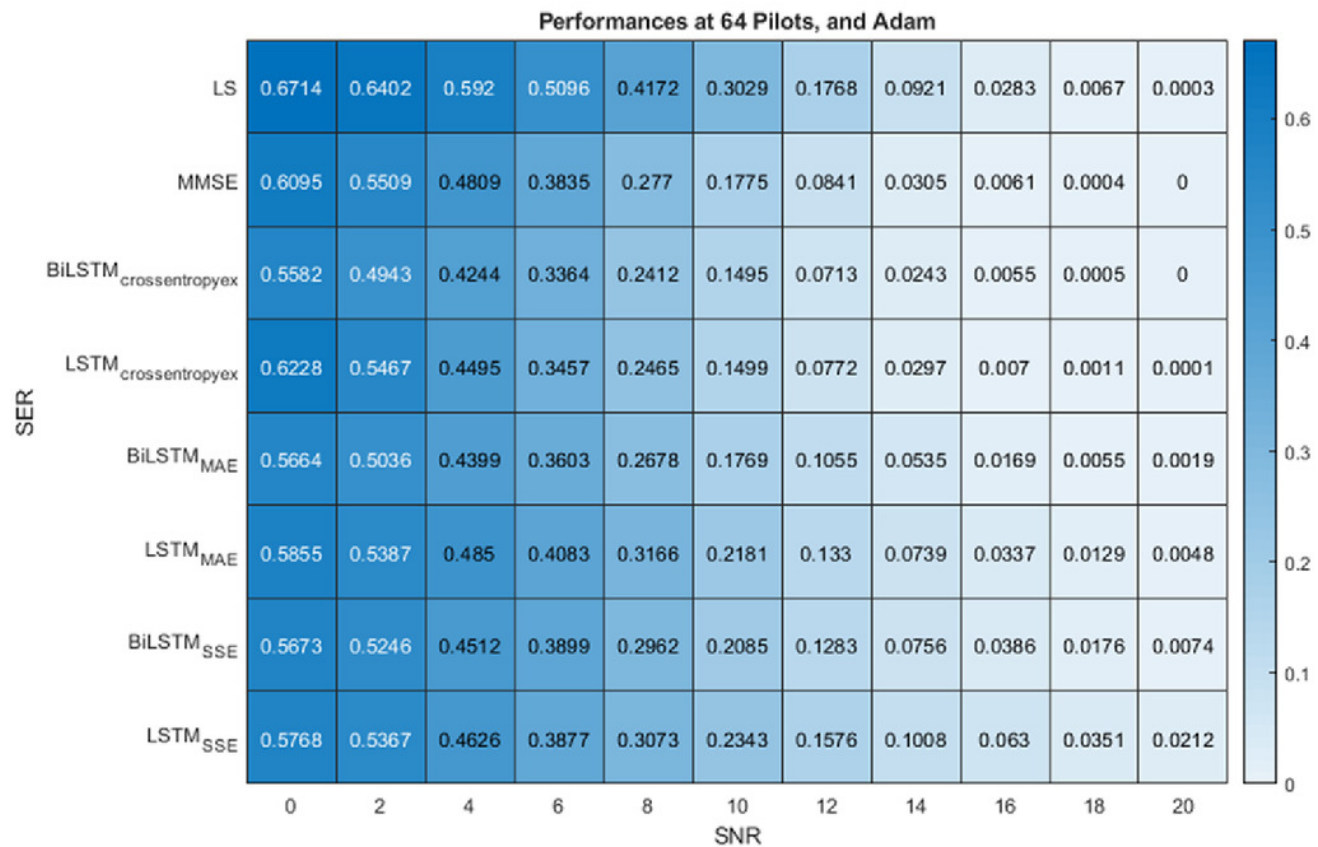


Figure 7

SER performance comparison of LS, MMSE, BiLSTM, and LSTM estimators using 8 pilots, the Adam learning algorithm and crossentropyex, MAE and SSE loss functions.

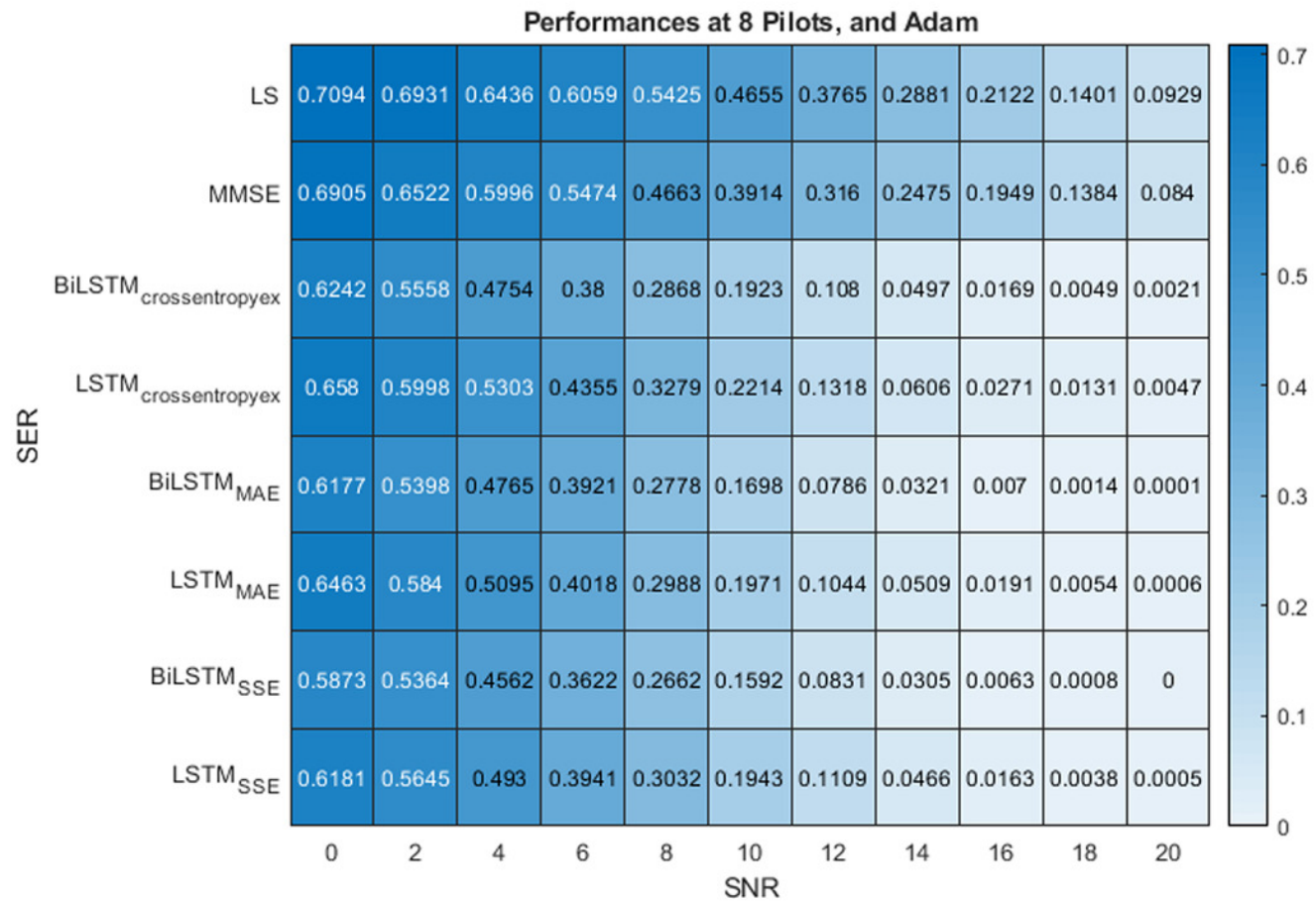


Figure 8

SER performance comparison of LS, MMSE, BiLSTM, and LSTM estimators using 4 pilots, the Adam learning algorithm and crossentropyex, MAE and SSE loss functions.

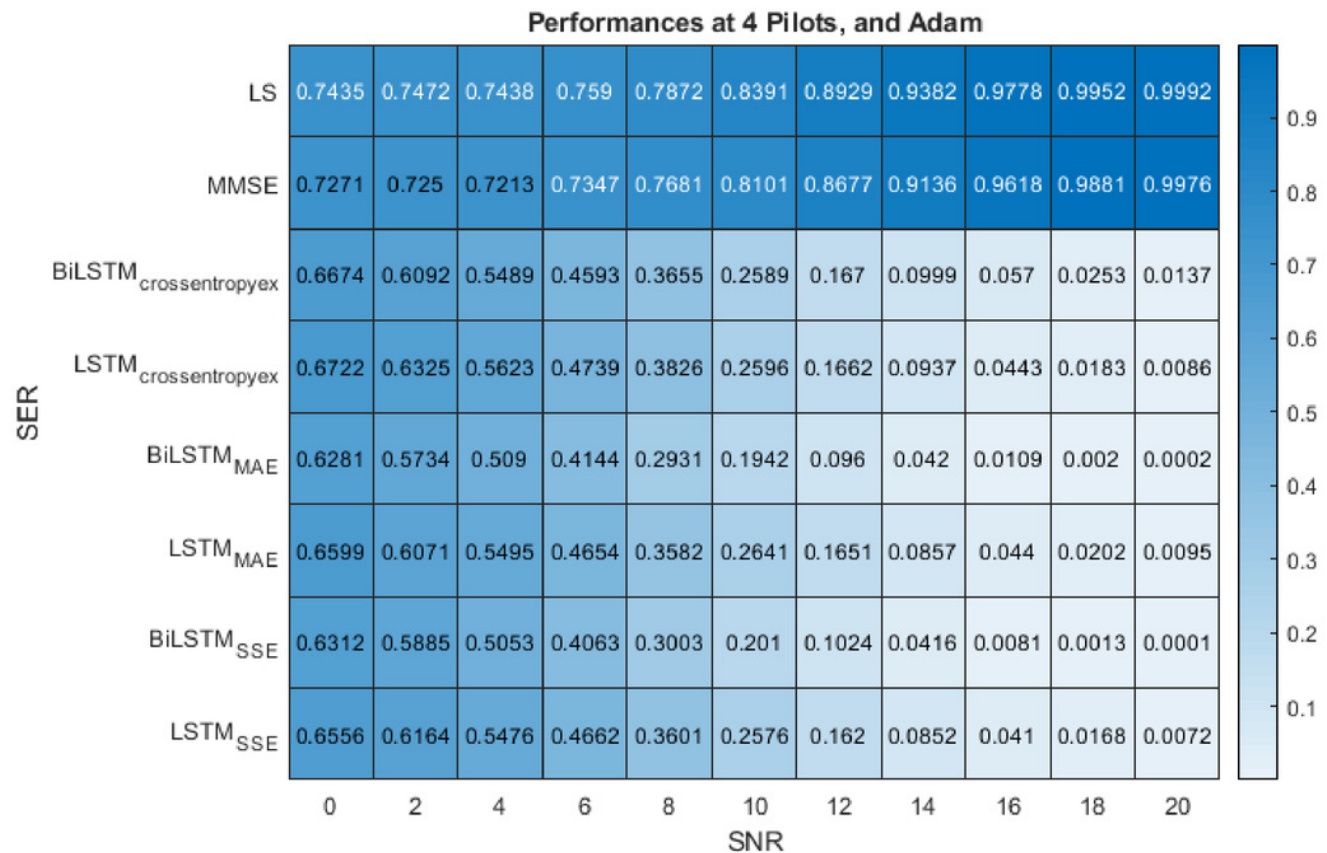


Figure 9

SER performance comparison of the best DL BiLSTM-based CSIEs using various pilots and loss functions.

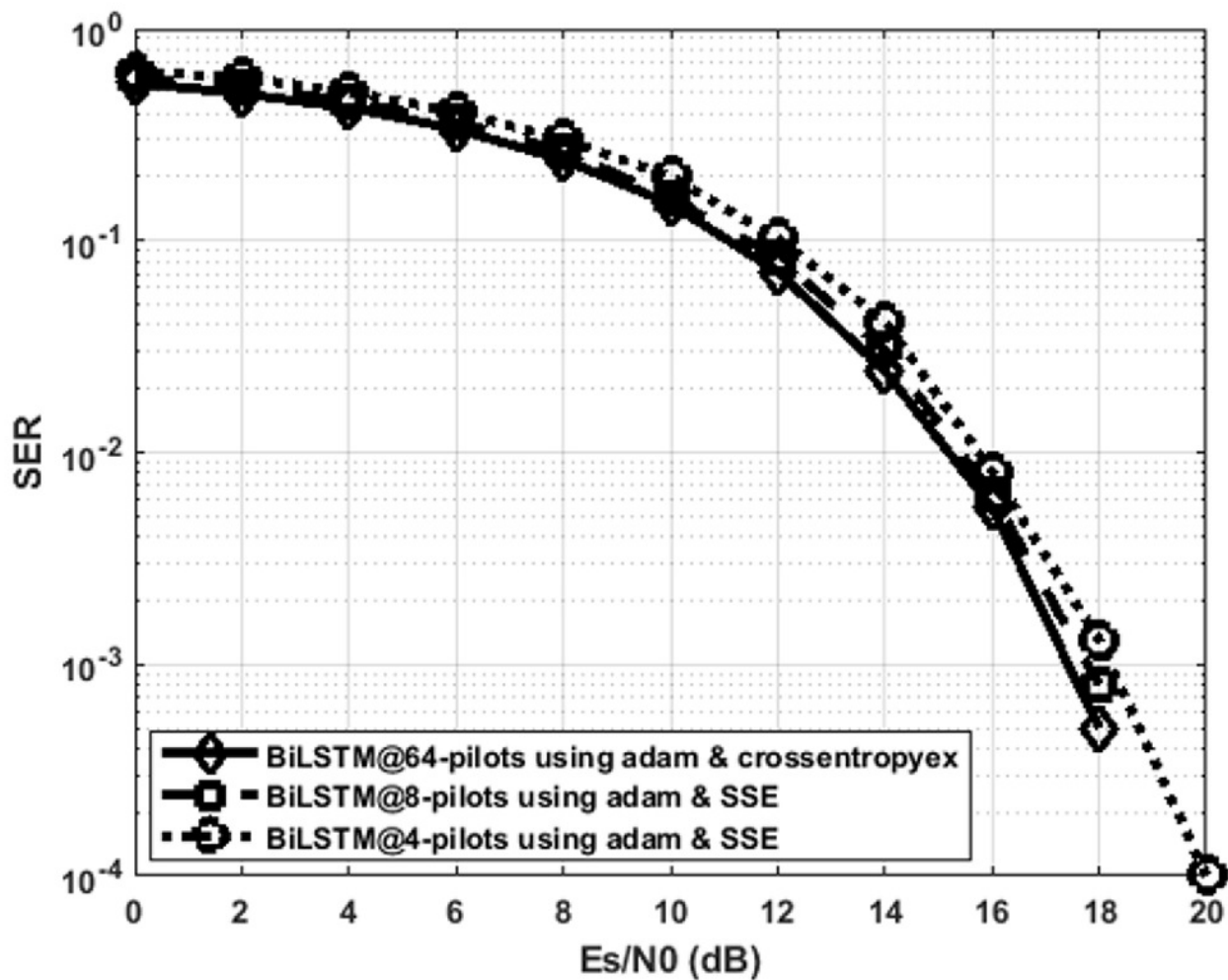


Figure 10

Loss curves comparison of BiLSTM- and LSTM- based estimators using 64 pilots, the Adam learning algorithm and crossentropyex, MAE and SSE loss functions.

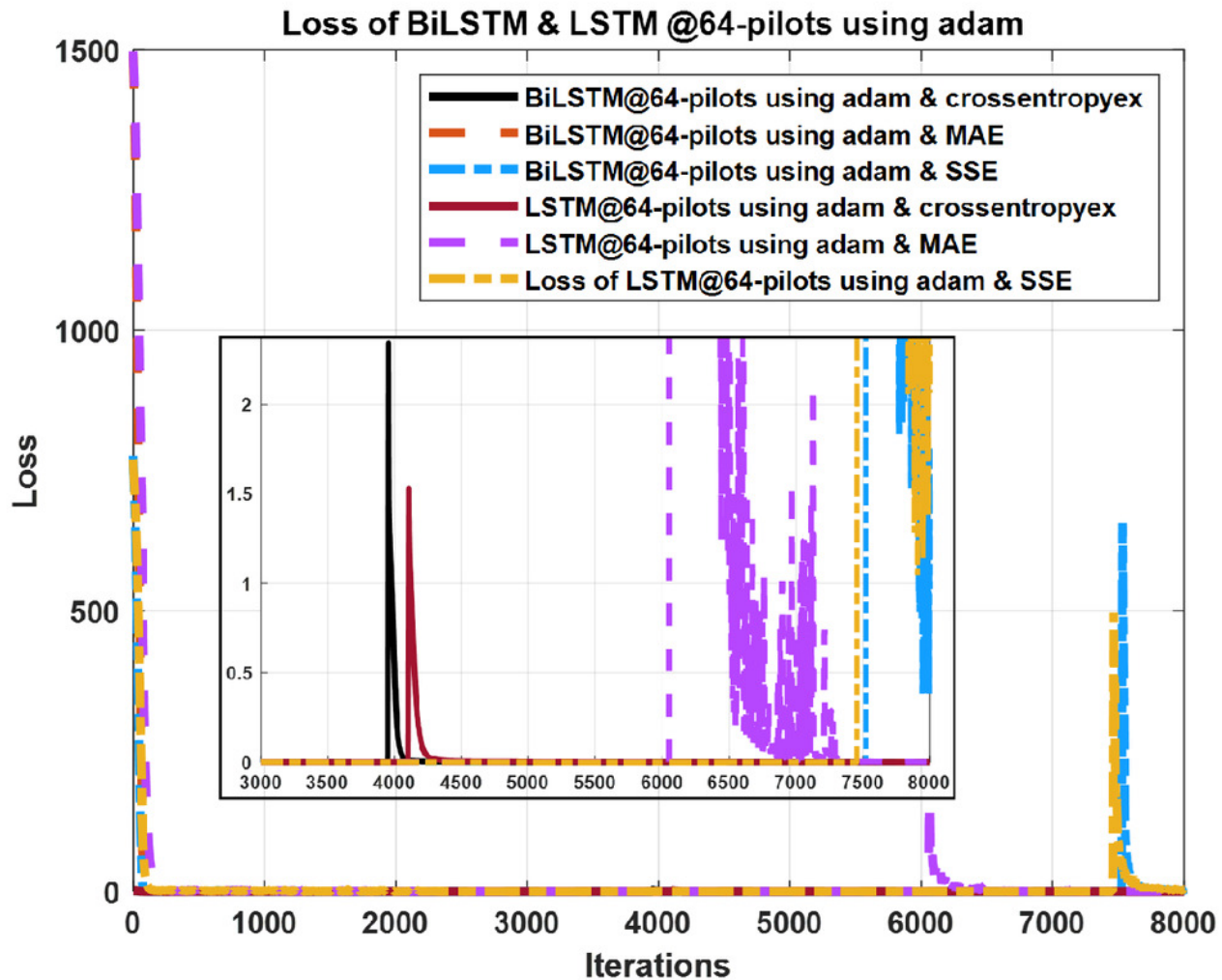


Figure 11

Loss curves comparison of BiLSTM- and LSTM-based estimators using 8 pilots, the Adam learning algorithm and crossentropyex, MAE and SSE loss functions.

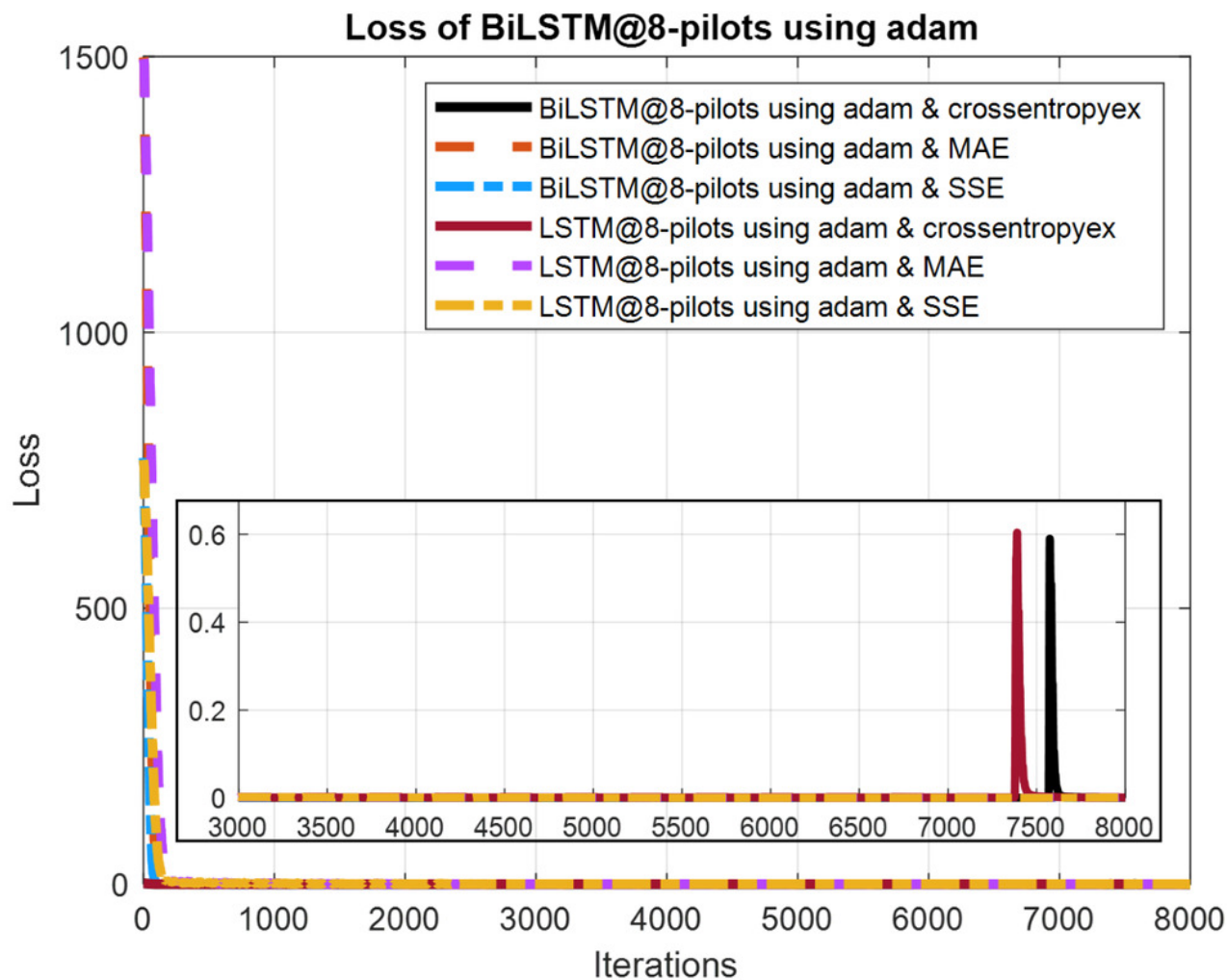


Figure 12

Loss curves comparison of BiLSTM- and LSTM-based estimators using 4 pilots, the Adam learning algorithm and crossentropy, MAE and SSE loss functions.

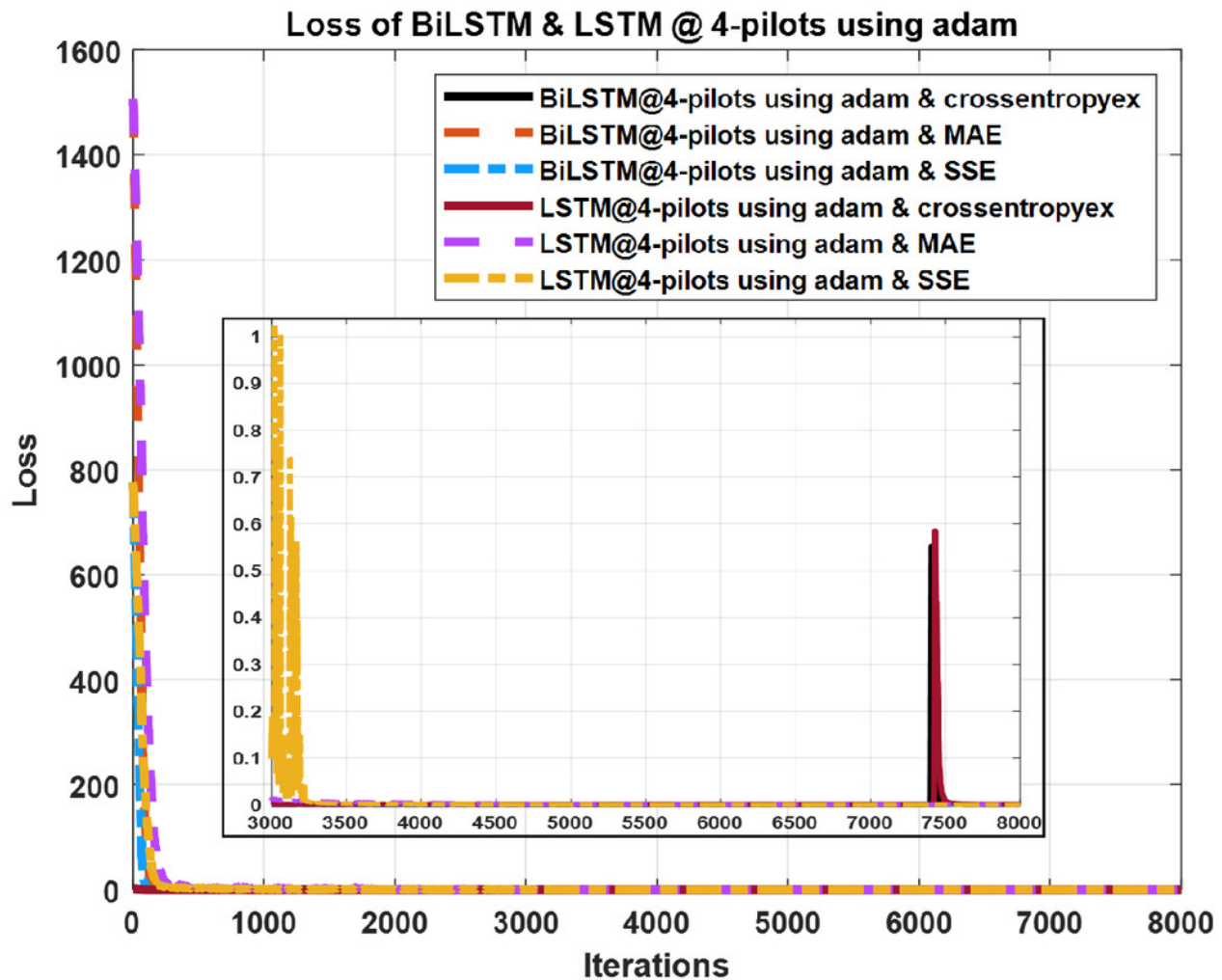


Figure 13

Performance comparison of BiLSTM-based estimator using 8 pilots, the RMSProp, SGdm, and Adadelta optimisation algorithms and crossentropyex, MAE and SSE loss functions.

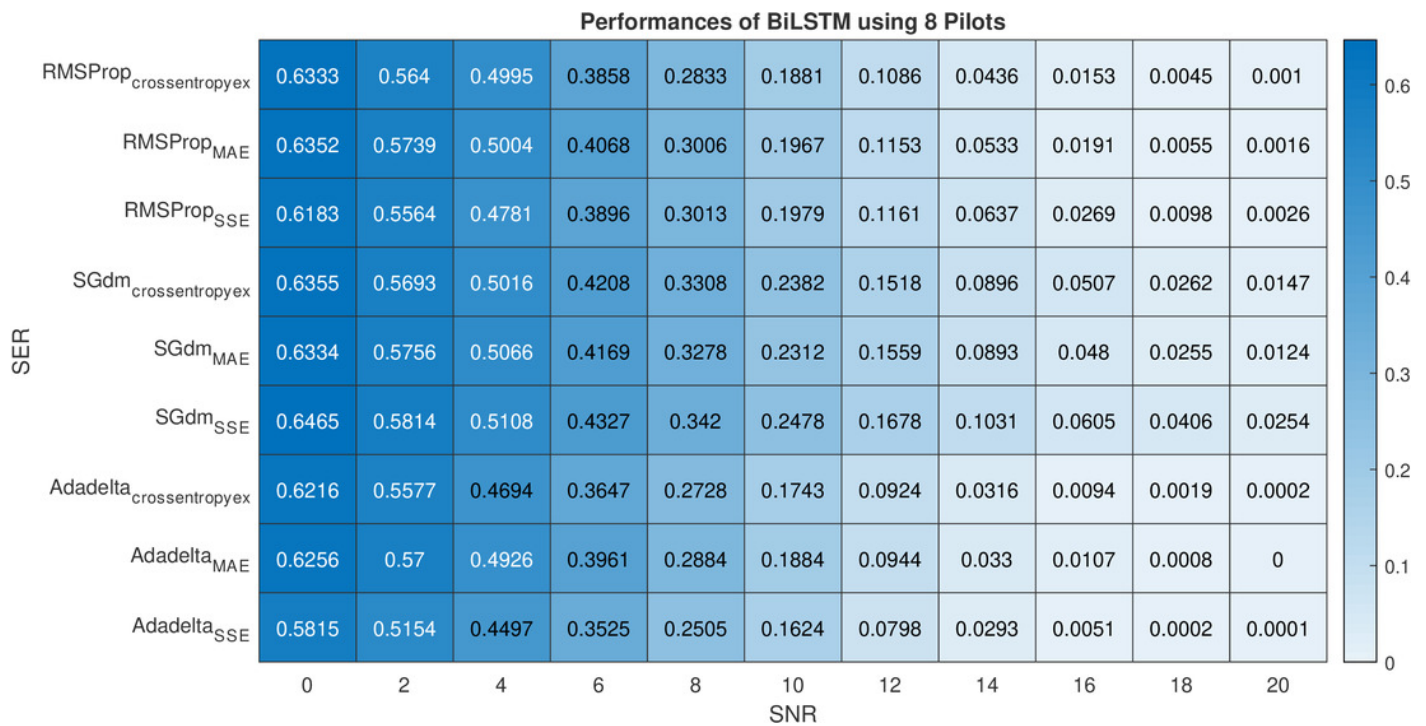


Table 1 (on next page)

BiLSTM- and LSTM-NN structure parameters and training process options

1
2
3
4
5
6
7
8

Parameter	Value
Input Size	256
BiLSTM Layer Size	30 hidden neurons
LSTM Layer Size	30 hidden neurons
FC Layer Size	4
Loss Functions	Crossentropyex, MAE, SSE
Mini Batch Size	1000
Epochs Number	1000
Learning Algorithm	Adam
Training Data Size	8000 - OFDM frame
Validation Data Size	2000 - OFDM frame
Test Data Size	10000 - OFDM frame

9
10
11
12
13
14
15
16
17
18
19
20
21
22
23
24
25
26
27
28
29
30
31
32
33
34

Table 2 (on next page)

OFDM system and channel parameters

1
2
3
4
5
6

Parameter	Value
Modulation Mode	QPSK
Carrier Frequency	2.6 GHz
Paths Number	24
CP Length	16
Subcarrier Number	64
Pilot Number	64, 8 and 4

7
8
9
10
11
12
13
14
15
16
17
18
19
20
21
22
23
24
25
26
27
28
29
30
31
32
33
34
35
36

Table 3 (on next page)

Accuracy comparison of the examined estimators using 64 pilots

1
2
3
4
5
6
7
8
9
10
11
12
13
14
15

64 pilots				
	BiLSTM	LSTM	MMSE	LS
Crossentropyx	100	99.99	100	99.94
SSE	99.23	97.88	100	99.96
MAE	99.87	99.52	100	99.97

16
17
18
19
20
21
22

Table 4 (on next page)

Accuracy comparison of the examined estimators using 8 pilots

1
2
3
4
5
6
7
8
9

8 pilots				
	BiLSTM	LSTM	MMSE	LS
Crossentropyx	99.84	99.53	91.34	91.62
SSE	100	99.95	91.60	91.49
MAE	100	99.94	91.53	91.50

10
11
12
13
14
15
16
17

Table 5 (on next page)

Accuracy comparison of the examined estimators using 4 pilots

1
2
3
4

5
6
7
8
9
10
11
12
13
14
15
16
17
18
19
20
21
22
23
24
25
26
27
28
29
30
31
32
33
34
35
36
37
38
39
40
41
42
43
44
45
46
47
48

4 pilots				
	BiLSTM	LSTM	MMSE	LS
Crossentropyex	98.61	97.94	0.24	0.02
SSE	100	99.28	0.24	0.09
MAE	99.97	99.05	0.26	0.04

Table 6 (on next page)

Performance comparison of different optimisation algorithms and its related accuracies

1
2
3
4
5
6
7
8
9
10

Order	Optimisation algorithm_{Loss function}	Accuracy
First	Adadelta_{SSE}	100%
Second	Adadelta_{crossentropyex}	99.99%
Third	Adadelta_{MAE}	99.98%
Fourth	RMSProp_{crossentropyex}	99.90%
Fifth	RMSProp_{MAE}	99.84%
Sixth	RMSProp_{SSE}	99.74%
Seventh	SGdm_{MAE}	98.76%
Eighth	SGdm_{crossentropyex}	98.53%
Ninth	SGdm_{SSE}	97.46%

11
12
13
14
15